



Article

An Optimal-Control Scheme for Coordinated Surplus-Heat Exchange in Industry Clusters

Brage Rugstad Knudsen * , Hanne Kauko and Trond Andresen 

SINTEF Energy Research, Kolbjørn Hejes vei 1B, 7491 Trondheim, Norway; hanne.kauko@sintef.no (H.K.), trond.andresen@sintef.no (T.A.)

* Correspondence: brage.knudsen@sintef.no

Received: 26 April 2019; Accepted: 13 May 2019; Published: 16 May 2019



Abstract: Industrial plants organized in clusters may improve their economics and energy efficiency by exchanging and utilizing surplus heat. However, integrating inherently dynamic processes and highly time-varying surplus-heat supplies and demands is challenging. To this end, a structured optimization and control framework may significantly improve inter-plant surplus-heat valorization. We present a Modelica-based systems model and optimal-control scheme for surplus-heat exchange in industrial clusters. An industry-cluster operator is assumed to coordinate and control the surplus-heat exchange infrastructure and responsible for handling the surplus heat and satisfy the sink plants' heat demands. As a case study, we use an industry cluster consisting of two plants with surplus heat available and two plants with heat demand. The total surplus heat and heat demand are equal, but the availability and demand are highly asynchronous. By optimally utilizing demand predictions and a thermal energy storage (TES) unit, the operator is able to supply more than 98% of the deficit heat as surplus heat from the plants in the industry cluster, while only 77% in a corresponding case without TES. We argue that the proposed framework and case study illustrates a direction for increasing inter-plant surplus-heat utilization in industry clusters with reduced use of peak heating, often associated with high costs or emissions.

Keywords: industry clusters; surplus-heat exchange; optimal control; thermal energy storage; energy efficiency; control of energy demand

1. Introduction

Heavy, carbon-intensive industries, such as cement, steel, iron, aluminum and petroleum refining, account for one-fifth of the global CO₂ emissions, without taking into consideration their electricity and heat demands [1]. These industries normally involve high-temperature processes with significant thermal-energy losses. The SPIRE association estimated in a report from 2013 [2] that approximately 20–50% of the energy used in industrial processes is lost as hot exhaust gases, cooling water and heat losses from equipment and products. As remedies, SPIRE has identified efficient heat recovery, reuse and conversion processes, and energy-storage technologies as prerequisites to reduce these losses. New energy-storage systems alone are targeted to contribute to 20–50% reduction in the energy use of industrial processes. Improving the ability to utilize industrial surplus heat, either within the plants themselves, in external plants or facilities or for district heating (DH), improves energy efficiency and reduces emissions related to heat provision.

To minimize loss in exergy, surplus heat should upon recovery be reused as close as possible to the heat source. For this reason, industrial companies often seek to utilize high-grade, high-temperature surplus heat within their plants, in particular within the process industries [3]. The opportunities to reuse remaining, lower grade surplus heat outside a plant depends highly on the specific industry, the temperature of the surplus heat and availability of suitable heat sinks. Industry clusters and

so-called eco-industrial parks where multiple plants from different industrial sectors are co-located in geographical proximity facilitates such utilization of surplus heat, as well as reuse of byproducts and waste water [4].

Efficient surplus-heat in industry clusters or across large process sites requires first establishing, designing and optimizing a heat-exchange network or infrastructure between a set of possible sources and sinks. This problem is closely related to total-site heat integration [5] and design of heat-exchanger networks (HENs) across multiple plants [6], and has been extensively studied, though little in the context of industry clusters [7]. Surplus heat often originates from off-gases or cooling of batch processes, yielding highly fluctuating, possibly non-continuous heat streams [8]. Long distances between the source and sinks may cause heat losses and together with time-varying demands cause difficulties for on-time heat supply [9]. In addition, the specifications for the heat exchange may change from the design-point of the HEN [10], e.g., due to changes in off-gas characteristics for the plant with surplus heat. Together, these conditions may cause severe operational challenges for efficient surplus-heat exchange in industry clusters despite a well-designed heat-exchange infrastructure. In this work, we address this latter operational problem. More precisely, we consider the challenge of optimally controlling the exchange of surplus heat across an industry cluster with time-varying and asynchronous availability and demand of heat, with strict heat-supply requirements and thermal energy storage (TES) to level out offsets in surplus heat and demand.

1.1. Related Work and Main Contribution

The problem we address in this paper lies at the intersection of utilization of surplus heat in industry clusters and between multiple plants (inter-plant heat exchange), optimal operation of HENs, and control of heat exchange with thermal storage. In this section, we give a brief review of some approaches and related work within these specific fields, focusing on control-related challenges.

The control and operational challenges of surplus-heat exchange in industry clusters bear resemblance with optimal operations of general HENs [11]. González et al. [12] developed a model predictive control (MPC) scheme for HENs on a linearized model. Bakošová and Oravec [13] developed a robust linear MPC scheme incorporating uncertainty in the heat-transfer coefficients and working-fluid density. Based on this work, Oravec et al. [14] developed a similar scheme for HENs with the objective of minimizing deterioration of the heat recovery caused by fouling of the heat exchangers (HEXs). Compared with proportional-integral (PI) control, they demonstrated that their proposed MPC potentially reduces heat losses and improves control performance. Meanwhile, Vasičkaninová and Bakošová [15] proposed a combined fuzzy and neural network predictive controller for a tubular HEX used in preheating of petroleum by hot water, using linear MPC based on a step-response model. Sun et al. [16] developed an MPC scheme for waste heat recovery in coke dry quenching processes using an artificial neural network. Wang et al. [17] considered proactive real-time reconfiguration of the optimal operation and control strategies of a HEN based on a steady-state model. All the above works apply either fuzzy models or discrete-time linear models and do not incorporate utilization of thermal storage.

While the above works resort to online optimal control approaches, other works have considered optimal operations of HENs by means of offline computations [18], seeking to maximize total heat transfer by computing and controlling the HEN at the optimal steady-state [19]. Scholten et al. [20] developed an internal model controller for a HEN incorporating TES for applications to district heating. Their approach, however, did not incorporate constraints in the exchange network or need for peak heating to cover the demand. Sun et al. [21] considered bypass control and economic optimization for HENs using a three-stage control-variable selection and adjustment approach, and demonstrated a potential for effective control and optimal economic operation. The topic of selecting optimally controlled variables in HENs was further analyzed by Jin et al. [22] to maximize the heat exchange amount. Bonilla and Roca [23] developed and experimentally tested a PI control loop for heat recovery from gas turbine exhaust gas, supplying a molten salt TES used in a renewable hybrid power plant.

Schumm et al. [24] considered hot water and steam mixing as a part of heat integration and recovery of low-temperature surplus heat in a cheese and whey powder plant, and developed a logic-based control scheme for the hybrid heat supply. Walmsley et al. [25] considered heat-recovery loops for inter-plant heat integration with use of solar heating, and applied conventional PI control for constant temperature set-point tracking of a TES unit. Other works have focused on technical control challenges related to industrial heat recovery such as Chen et al. [26] who analyzed optimal simultaneous operations for pumps and valves in HENs under variable heat loads, and Sunil et al. [27] who developed a robust feedback controller based on frequency domain analysis for a heat recovery steam generator with integration of renewable energy. Common for the above references is that they either target optimal steady-state operations or control of varying heat streams by means of disturbance rejection assured through proper control design, and do not incorporate constraints in the heat-exchange infrastructure or seek to exploit TES for minimizing additional heat acquisition needed to meet the demand.

Related to the handling of time-varying surplus-heat streams, several works have studied the dynamic response of HENs and related issues arising from transients in the heat streams. Atkins et al. [28] performed transients' stream analysis for inter-plant heat integration at a dairy factory and considered effects of thermal storage volume and temperatures of hot and cold loops. They concluded that good control was important to maximize effective storage of the tank and heat recovery. Wang et al. [29] developed a linear state-space model for controller design of plate HEXs to enable stable and efficient operations of heating substation in DH networks. Whalley and Ebrahimi [30] presented a general dynamic modeling process for tube and shell HEXs, with associated feedback control design techniques. These studies have developed control-relevant models, but do not directly optimize the control inputs or address constrained control.

Meanwhile, a few studies have considered control issues in conjunction with the design of HENs, or infrastructure and utility systems for inter-plant or site-wide heat integration. Chang et al. [31] considered the design of HENs for indirect inter-plant heat integration with the objective of improving the control and degree of operational flexibility, using a game-theoretic approach. Gu et al. [32] presented a method to incorporate flexibility and controllability measures in the synthesis of HENs to maintain optimal operations in the presence of disturbances. Čuček et al. [33] considered challenges and approaches for retrofitting HENs within industrial sites. They identified real-time optimization and process control as a future challenges for retrofitting HENs in existing processes and across total sites. Jimenez-Arreola et al. [10] reviewed challenges related to handling fluctuations in the off-gas temperature for waste-heat to power systems, describing the need for proper control of TES and steam control to achieve high efficiency and stable operations. Schlosser et al. [34] used Monte Carlo simulations for robust design and operations of heat-recovery loops, including a multi-mode logic-based PI controller for a stratified storage tank. Finally, we note that several studies have considered the isolated problem of optimal design of infrastructure and utility systems for plant-wide or inter-plant heat integration—see, e.g., [35,36].

In view of the above referred literature, there are few, if any, studies that address the system-level operational challenges and constrained control of heat exchange in industry clusters. In particular, there is a lack of control schemes for optimal dynamic operations of TES units that effectively enables hedging against time variations and offsets in demand and supply, incorporate constraints in the heat-exchange infrastructure, and heat-supply requirements at the demand side. For this purpose, optimal-control schemes that directly incorporate the possibly nonlinear dynamics of the heat-exchange infrastructure and exploit predictions in surplus-heat streams and demand is an attractive approach, as well as a key part of online optimization of surplus-heat exchange in industry clusters. Such schemes may reduce heat-acquisition costs for industrial plants, improve energy efficiency in industry clusters, and reduce use of fossil-fuel based peak heating often causing high CO₂ emission rates. Our main contribution is a novel sparsity-promoting optimal-control formulation that optimizes the available control actuation and thermal capacities of the heat-exchange infrastructure to supply a given, time-varying heat demand to plants in the industry cluster at minimal use of peak heating.

The proposed framework applies to industry cluster operators both with and without TES units; we demonstrate and quantify the benefits of integrating TES and optimization-based control in order to fully utilize the energy-storage facilities.

1.2. Outline

The remainder of the paper is organized as follows: Section 2 defines the problem studied in the paper. Section 3 describes the applied methodology, with a system-modeling approach for inter-plant heat exchange in industrial clusters in Section 3.1 followed by description of the proposed optimal-control scheme in Section 3.2. A numerical case study is presented in Section 4 to assess the proposed methodology. Concluding remarks in Section 5 complete the paper.

1.3. Notation

The terms “industry park” and “industrial cluster” are interchangeably used in describing a set of co-located industrial plants, with “eco-industrial parks” as a recurring denotation of industrial parks/clusters that exchange resources to decrease energy use or environmental footprint—see, e.g., [37]. In this paper, we use the term industry cluster to describe a set of industrial plants located in geographical proximity, seeking to utilize and exchange common resources.

We use a bar over letters to indicate the value is a parametric input and not a variable in the optimal-control problems. Furthermore, we use bold letters for vectors, and a dot for time derivatives. Sets and indices are given in Table 1, while a list of nomenclature and abbreviations is included at the end of paper.

Table 1. Sets and indices.

| Index | Interpretation | Set | Elements |
|-------|--------------------------|---------------|----------------------|
| i | Plants with surplus heat | \mathcal{I} | $\{1, 2, \dots, I\}$ |
| j | Plants with heat demands | \mathcal{J} | $\{1, 2, \dots, J\}$ |

2. Problem Description

This section introduces the surplus-heat exchange system for a generic industry cluster, together with the associated coordination or control problem. Consider Figure 1, illustrating an industry-cluster topology for surplus-heat exchange with a TES unit. The industry cluster consists of a set \mathcal{I} source plants with surplus heat which they are unable to utilize within their individual plants, and a set \mathcal{J} plants or sinks with heat demands. Both the available surplus heat and the demands may be highly time varying. We denote the surplus-heat streams $\bar{Q}_i^{\text{source}}(t)$ for each plant $i \in \mathcal{I}$, and the heat demands $\bar{Q}_j^{\text{demand}}(t)$, $j \in \mathcal{J}$. Both the supplies and demands are formulated as parametric inputs to the system, i.e., they are given, possibly time-varying quantities. We assume that the heat streams from each source i are sufficiently clean (scrubbed) to be supplied through a heat exchanger connected to a supply pipeline.

In the industry cluster, we assume that an operator, coordinator or park authority operates the infrastructure for the surplus-heat exchange, cf. Figure 1. The cluster operator’s main task is to coordinate the time-varying, possibly asynchronous surplus-heat supplies and demands. In particular, the operator must deliver the demanded heat to the sink plants subject to certain contracted quality specifications, given by a temperature and allowed deviation from the demand heat-flow rate $\bar{Q}_j^{\text{demand}}(t)$. The operator controls a set of pumps for the heat supply and a set of peak heat-supply units. Peak-heating units are typically boilers using fossil fuels or electricity [38]. Consequently, minimizing the use of these units is advantageous from both economical and environmental perspectives. For this, we formulate the following problem definition:

Problem 1. Given a planning period $[t_0, t_f]$, available surplus heat-flow rates $\bar{Q}_i^{\text{source}}(t)$ from a set of source plants $i \in \mathcal{I}$, heat-flow demands $\bar{Q}_j^{\text{demand}}(t)$ for the sink plants $j \in \mathcal{J}$, and a set of quality requirements for the heat supply, minimize the necessary peak-heating supply for meeting the demands from the sink plants \mathcal{J} .

We confine the study to industry clusters where the plants are located up to a few hundred meters apart. Furthermore, we consider water as energy carrier, although the framework is extendable to other heat-transfer fluids, e.g., steam, upon certain modifications. The framework may adopt both long and short time scales for the coordination of surplus-heat exchange. We focus the control problem on horizons ranging from a few hours to a couple of days, where heat availabilities and demands change on a 15–30 min basis or less frequently.

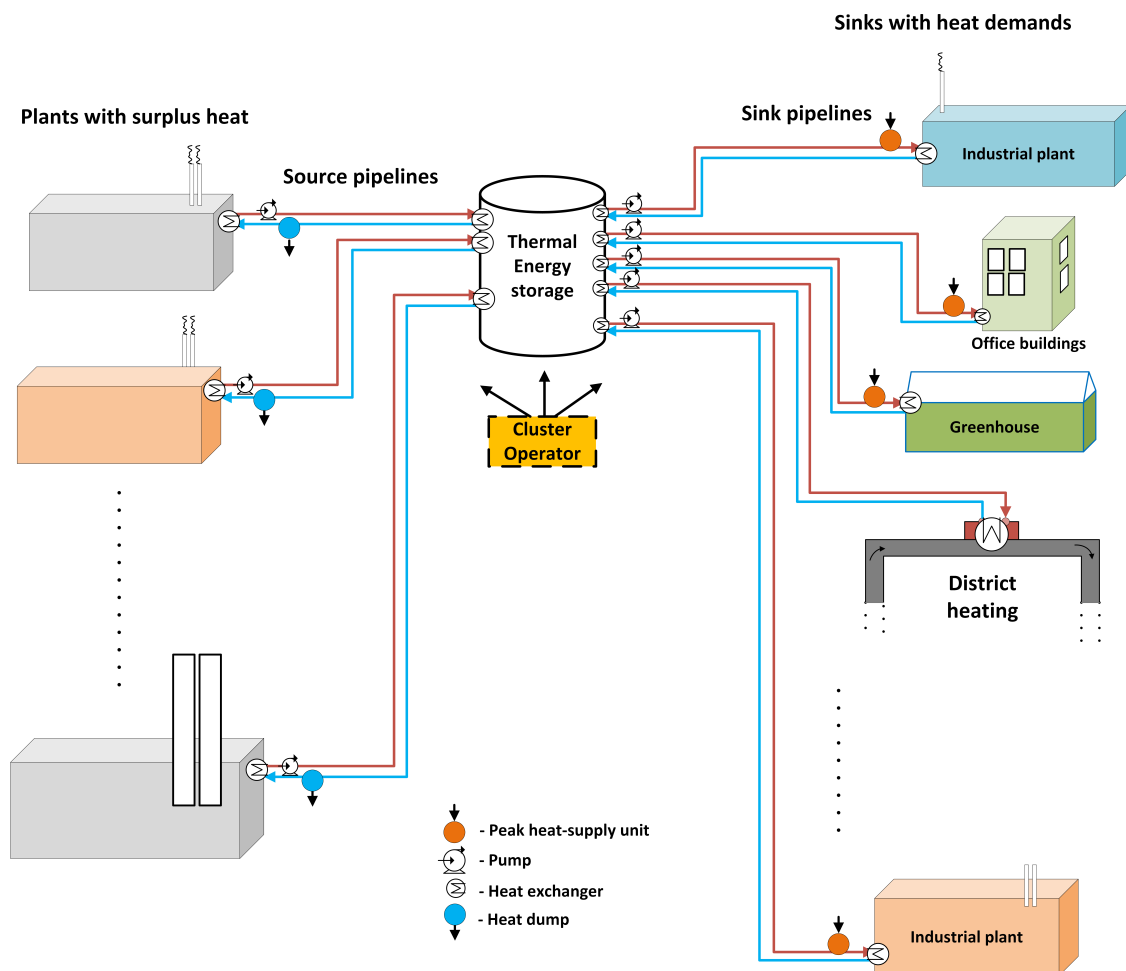


Figure 1. Conceptual illustration of surplus-heat exchange and utilization in an industry cluster. The red lines indicate hot supply water and blue lines cold return water.

3. Methodology

3.1. Systems Modeling of Surplus-Heat Exchange in Industrial Clusters

Modeling of industrial clusters may be a formidable task, facing inherently complex and dynamic processes with many levels of integration. In order to incorporate the relevant processes and dynamics in the model, the modeling and detail level must reflect the scope of the model. For the purpose of systems modeling of heat-exchange infrastructure in industry clusters, we apply the open-source, equation-based modeling language Modelica [39]. Modelica is object oriented, providing high modularity, reusability and adaptability of the created model-components, and has been proven to be a flexible and efficient modeling tool for many energy systems [40–42]. Being an equation-based

or acausal modeling language [43], Modelica relieves the user from specifying inputs and outputs of each submodel and transforming the submodels to a complete differential-algebraic equations (DAEs) for numerical integration. For a comparison with other modeling and simulation environments such as Simulink and TRNSYS, see, e.g., [44].

Object-oriented modeling of the surplus-heat exchange infrastructure depicted in Figure 1 requires constructing unit models (classes) for pipelines, heat exchangers, thermal-energy storage, pumps, heat sources and sinks. While explicit formulation of the governing differential equations for these units may be implemented, the object-oriented structure enables formulation of the required model classes by means of inheriting and interconnecting a set of basic low-level components. Each component obeys energy and mass balances, and is equipped with input and output ports. This enables full exploitation of object-oriented energy-systems modeling and a consistent model structure, however, with a possible cost of added overhead in simulation time. We describe in this section the main elements of the chosen systems model to illuminate the detail level of the different parts of the thermal grid, its connections, boundary conditions and selection of dynamic and static components. For readability, we summarize in Table 2 the variables of the system model.

Table 2. Variables of system model and optimal-control problem.

| Variable | Description | Unit |
|-----------|-----------------------------------|-------------------|
| Q | Heat-flow rate | kW |
| T | Temperature | K |
| u | control input | [-] |
| \dot{V} | Volumetric flow rate | m ³ /s |
| z | Algebraic state of pipeline model | - |

On the source side of the industry cluster in Figure 1, we define as boundary conditions the available surplus heat $\bar{Q}_i^{\text{source}}(t)$ as the the heat duty delivered through the depicted heat exchangers. The surplus heat from each source plant is transported through a source water-pipeline, which can essentially be represented as a discretized one-dimensional heat equation [45] with a static pressure-loss map. The flow of the heat-exchange fluid is driven by pumps. We denote the resulting DAEs as

$$\mathbf{F}_i(t, \dot{\mathbf{T}}_i^{\text{pipe-source}}(t), \mathbf{T}_i^{\text{pipe-source}}(t), \mathbf{z}_i^{\text{pipe-source}}(t), \bar{Q}_i^{\text{source}}(t), Q_i^{\text{TES,in}}(t), Q_i^{\text{loss}}(t), Q_i^{\text{hd}}(t)) = 0, \quad i \in \mathcal{I}, \quad (1a)$$

$$\mathbf{T}_i^{\text{pipe-source}}(0) = \mathbf{T}_i^{\text{pipe-source,init}}, \quad i \in \mathcal{I}, \quad (1b)$$

where $\mathbf{F}_i(\cdot)$ are vector-valued functions which arguments t is time, \mathbf{T}_i an n^p -dimensional vector of temperatures, $\mathbf{z}_i^{\text{pipe-source}}(t)$ a vector with algebraic states, $Q_i^{\text{TES,in}}(t)$ the heat-flow rate from pipeline to storage tank through a heat exchanger, and $Q_i^{\text{loss}}(t)$ heat losses from the pipelines. The final set of algebraic states $\mathbf{z}_i^{\text{pipe-source}}(t)$ depends on the model accuracy and use of state-dependent parameters, but typically consists of the pipe inlet and outlet pressers, fluid enthalpy and flow velocity. We omit modeling of the cooling circuits in the source plants, and simply assume that each plant $i \in \mathcal{I}$ requires the return water on the heat-exchanger cold side to be below a certain maximum temperature and circulated at a constant flow velocity. To ensure this, we include in Equation (1) a variable heat-flow rate $Q_i^{\text{hd}}(t)$ which enables the operator to dump (or reject) heat to a cold reservoir.

For applications of optimal control for surplus-heat exchange with thermal storage, the primary characteristics of a TES model are the total storage capacity, and charging and discharging times. Several TES technologies and variants exist, and the suitable and economically viable choice of storage technology depends on the capacity, charge and discharge requirements [46]. We consider sensible TES by means of a hot water tank. In practice, hot water tanks will exhibit stratification due to density difference along the vertical temperature gradient [47]. Thermal stratification is generally a complex physical process [48]. To retain a sufficiently simplified numerical systems model, we assume a uniform mixing throughout the tank and thus omit modeling of stratification in the tank. An indirect

heat-transfer scheme between the tank and the supply and sink pipelines is applied, using a set of heat exchangers. We further assume that the tank is not pressurized, thereby leading to the simple TES model

$$\rho c^w V^{\text{TES}} \dot{T}^{\text{TES}}(t) = \sum_{i \in \mathcal{I}} Q_i^{\text{TES},\text{in}}(t) - \sum_{j \in \mathcal{J}} Q_j^{\text{TES},\text{out}}(t) - Q^{\text{TES},\text{loss}}(t), \quad (2a)$$

$$T^{\text{TES}}(0) = T^{\text{TES},\text{init}}, \quad (2b)$$

where ρ and c^w are density and specific heat capacity of water, respectively, V^{TES} the tank volume, $T^{\text{TES}}(t)$ the assumed uniform storage temperature, $Q_i^{\text{TES},\text{in}}(t)$ and $Q_j^{\text{TES},\text{out}}(t)$ the heat-flow rates in and out of the TES unit, respectively, and $Q^{\text{TES},\text{loss}}(t)$ heat losses to the ambient, given by

$$Q^{\text{TES},\text{loss}}(t) = (UA)^{\text{loss}} (T^{\text{TES}}(t) - T^{\text{amb}}(t)), \quad (3)$$

where $T^{\text{amb}}(t)$ is ambient temperature, U overall heat-transfer coefficient and A heat-transfer area. As design criteria, we specify a desired heat duty that the hot-water tank should deliver per hour subject to a given temperature drop and no heat supply, thereby giving the total volume of the tank. A hot water tank or accumulator is only one option for TES; the modularity of the proposed object-oriented systems model allows the simple model (2) and (3) to be extended or replaced by more complex sensible TES models, possibly with other working fluids and heat-transfer configurations, however, at the cost of increased numerical complexity (e.g., [49])

We use a discretization approach to model the HEXs between the source pipelines and the TES unit. For this purpose, we discretize the hot side of the HEX into n^{HEX} hydraulic segments and connect a thermal conductor to each segment. While the heat capacitance of the pipelines is important to include in the model, the heat-transport delay from source to sink is generally less important, comparing that the pipeline lengths in industry clusters are normally limited to some hundred meters, cf. Section 2. To limit the model size, we hence connect each of the n^{HEX} conductors to a segment of the source pipeline, leading to the heat-transfer model

$$Q_i^{\text{TES},\text{in}}(t) = \sum_{k=1}^{n^{\text{HEX}}} (UA)_{ik} (T_{ik}(t) - T^{\text{TES}}(t)), \quad i \in \mathcal{I}. \quad (4)$$

Observe that the products $(UA)_k$ are computed independently of the pipeline volumes to which they are coupled, and are thus unaffected by this model simplification. Offline computation of total UA values for each discretized HEX is performed by evaluating the basic heat-balance equation for a nominal log-mean-temperature-difference (LMTD) and a desired heat-flow rate. However, for numerical robustness of the online model evaluations, we use the minimum temperature approach in the heat balance equations instead of LMTD evaluations to prevent HEX temperature crossings. In general, we choose $n^{\text{HEX}} < n^p$, that is, we apply more segments for the discretized pipeline compared to the discretized HEXs. Alternative models to Equation (4) are the NTU model or LMTD approximations—see, e.g., [50].

The model of the sink pipelines is similar to the model (1) of the source pipelines, and stated implicitly as a set of DAEs

$$\mathbf{G}_j \left(t, \mathbf{T}_j^{\text{pipe-sink}}(t), \mathbf{T}_j^{\text{pipe-sink}}(t), \mathbf{z}_j^{\text{pipe-sink}}(t), Q_j^{\text{TES},\text{out}}(t), Q_j^{\text{loss}}(t), \dot{V}_j^{\text{pump}}(t) \right) = 0, \quad j \in \mathcal{J}, \quad (5a)$$

$$\mathbf{T}_j^{\text{pipe-sink}}(0) = \mathbf{T}_j^{\text{pipe-sink,init}}, \quad j \in \mathcal{J}. \quad (5b)$$

For the vector-valued functions $G_j(\cdot)$ in (5), $\mathbf{T}_j^{\text{pipe-sink}}(t)$ is an n^p -dimensional vector of temperatures in the discretized pipeline, $\mathbf{z}_j^{\text{pipe-sink}}(t)$ a vector of algebraic states, $Q_j^{\text{TES},\text{out}}(t)$ the heat-flow rate from

the tank, $Q_j^{\text{loss}}(t)$ aggregated heat losses from the sink pipelines, and $\dot{V}_j^{\text{pump}}(t)$ the controllable pump flow-rate.

For the heat exchange between the TES unit and the sink pipelines in Figure 1, we use a single-element pipe with a connected thermal conductor to model $Q_j^{\text{TES,out}}(t)$. The HEXs between the sink pipelines and sink plants in Figure 1 are modeled by a similar discretization approach as described above for the heat inflow (4) to the TES unit. The sink plants' utilization of the supplied heat is controlled by the plants themselves and not by the industry cluster operator. Consequently, we define as boundary condition on the sink side a fixed temperature \bar{T}_j^{sink} at which the heat-flow rate $\bar{Q}^{\text{demand}}(t)$ should be delivered. Note that, for notational convenience, we apply an equal number of elements for all discretized HEXs and pipelines, respectively, while these numbers are set independently in the model implementation.

Finally, the model of the industry cluster includes a set of peak-load units, indicated with orange dots in Figure 1. Wang et al. [51] demonstrated that peak-load units in DH systems that acquire electricity at a market price should be located close to sinks with dense heat demands to achieve high energy efficiency. As such, we assume that a set peak-load or peak-heating units are distributed close to the sink plants, and hence remotely controlled by the cluster operator. The control of these peak-heating units will be addressed in the sequel.

3.2. Optimal-Control for Coordinated Surplus-Heat Exchange

Efficient utilization of multi-stream, possibly time-varying surplus heat in complex industry clusters requires structured control and optimization solutions. For cluster operators, the operational challenges involve satisfaction of demands, ensuring sufficient cooling of the sources processes, safety of operations, sufficiently high revenue of its services, as well as resilience against contingencies such as time-limited drop-outs of one or several heat sources [52]. A structured optimal-control strategy may alleviate these operational challenges by leveraging predicted variations in heat demand and supply, utilization of the thermal storage capacities, and by enabling operations close to the constraints of the infrastructure. In the sequel, we describe a framework for optimal control of coordinated surplus-heat exchange in industry clusters.

3.2.1. Control Variables

To satisfy the heating demand from the sink plants, the cluster operator controls the pump volumetric flow-rate $\dot{V}_j^{\text{pump}}(t)$ for circulating the water in the sink pipelines, and the heat-flow rate $Q_j^{\text{peak}}(t)$ from the set of distributed peak-heating units, cf. Figure 1. Observe that we use, by convention, $\dot{V}(t)$ to denote the pump's volumetric flow-rate, while these are control variables and not time-derivatives of states. As stated in Section 3.1, we assume that constant-flow pumps circulate the water in the source-plant pipelines, but that the operator may dump heat at a rate $Q_i^{\text{hd}}(t)$ to ensure that the return-water temperature in these circuits is below a certain threshold. This leaves the vector of control (inputs) variables

$$\mathbf{u}(t) := \left[\dot{V}_1^{\text{pump}}(t), \dot{V}_2^{\text{pump}}(t), \dots, \dot{V}_J^{\text{pump}}(t), \right. \\ \left. Q_1^{\text{peak}}(t), Q_2^{\text{peak}}(t), \dots, Q_J^{\text{peak}}(t), \right. \\ \left. Q_i^{\text{hd}}(t), Q_2^{\text{hd}}(t), \dots, Q_I^{\text{hd}}(t) \right]'. \quad (6)$$

The control variables (6) are subject to the constraints

$$0, \leq \dot{V}_j^{\text{pump}}(t) \leq \bar{\dot{V}}_j^{\text{pump}}, \quad j \in \mathcal{J}, \quad (7a)$$

$$0, \leq Q_j^{\text{peak}}(t), \quad j \in \mathcal{J}, \quad (7b)$$

$$0, \geq Q_i^{\text{hd}}(t), \quad i \in \mathcal{I}. \quad (7c)$$

Remark 1. Peak heating may be supplied from different energy sources, including both fossil fuel, biofuel and electricity. In practice, there will always be an upper bound on the power supply, and possibly on the ramping rate. In continuous-time optimal-control problem, the latter requires defining an auxiliary state and differentiate the control variable $Q^{\text{peak}}(t)$, which is numerically disadvantageous. For the purpose of this study, we hence omit such constraints.

3.2.2. Constraints

We assume that the cluster operator is obligated to supply each sink plant $j \in \mathcal{J}$ with a heat-flow rate $Q_j^{\text{del}}(t)$ within a certain contracted range of the demanded heat-flow rate $\bar{Q}_j^{\text{demand}}(t)$. For this satisfaction of demand, we define

$$Q_j^{\text{del}}(t) := Q_j^{\text{TES,out}}(t) - Q_j^{\text{loss}}(t) + Q_j^{\text{peak}}(t), \quad j \in \mathcal{J}, \quad (8)$$

with the constraints

$$\left| Q_j^{\text{del}}(t) - \bar{Q}_j^{\text{demand}}(t) \right| \leq \delta_j \bar{Q}_j^{\text{demand}}(t), \quad j \in \mathcal{J}, \quad (9)$$

where the parameter $\delta_j \in [0, 1]$ decides how strictly the delivered heat-flow rate must be met relative to the demand. From an economical perspective, a low value of δ_j means that the operator may require a higher price for the heat delivered to the sink plants. Typical values of δ_j may be 0 to 0.05, allowing a slack of up to 5% between the demanded and delivered heat-flow rate to each sink plant $j \in \mathcal{J}$.

There may be numerous operational constraints in the surplus-heat exchange infrastructure, both safety and performance related. Assuming that the hot-water storage tank is unpressurized, to avoid boiling the temperature of the storage tank must not exceed an upper level $T^{\text{TES,max}}$, i.e.,

$$T^{\text{TES}}(t) \leq \bar{T}^{\text{TES,max}}. \quad (10)$$

The return temperature in the source pipeline, denoted $T_{j,p}^{\text{pipe-source}}$ and hence the last element of the vector $T_i^{\text{pipe-source}}(t)$, is upper bounded by $\bar{T}_i^{\text{source,C}}$,

$$T_{i,p}^{\text{pipe-source}}(t) \leq \bar{T}_i^{\text{source,C}}, \quad i \in \mathcal{I}. \quad (11)$$

Recall that we assume a fixed temperature (system boundary condition) at the cold side of HEXs between the sink pipelines and the sink plants. We do not enforce further constraints on the source or sink pipelines, while any additional constraints may easily be added.

3.2.3. Objective Function

The primary control objective for the cluster operator is to minimize the use of peak-heating supply to satisfy the demands (9). Both the cost and emissions of running peak-load units may vary as a function of the load and during ramping [53]. As such, the objective function lends itself both to economical and environmental considerations rendering different, possibly conflicting criteria. In this study, we define the following objective function:

$$\min_{\mathbf{u}(t)} \int_{t_0}^{t_f} \left(\sum_{j \in \mathcal{J}} Q_j^{\text{peak}}(t) + \gamma_1 \sum_{i \in \mathcal{I}} Q_i^{\text{hd}}(t)^2 + \gamma_2 \sum_{j \in \mathcal{J}} v_j^{\text{pump}}(t)^2 \right) dt. \quad (12)$$

The first term of the Lagrange integrand in (12) minimizes the total peak-load energy use during the prediction horizon from t_0 to t_f , and yields an L_1 cost function due to the nonnegativity constraints (7b). The second and third terms penalize the two other sets of control variables by means of quadratic costs. Dumping of heat from the source-pipe return water causes waste of energy and should be avoided unless necessary to obey the constraints (10). However, these two quartic terms are primarily introduced for regularization, in order to avoid ill-conditioned singular control

problems—see Biegler [54] (Chapter 10). Upon sufficient scaling of the variables in (12), we hence choose the non-negative parameters γ_1 and γ_2 such that $\gamma_1 \leq \gamma_2 \ll 1$. The prediction horizon t_i must be selected sufficiently long to incorporate the dominating dynamics of the heat-exchange infrastructure and the time variations of the surplus heat and demands, while also short enough to retain numerical efficiency. Observe that the last term of (12) may be argued to implicitly account for the energy use of the pumps.

Imposing the heat-flow rates from the peak-load units in (12) as an L_1 criteria promotes sparse solutions [55]. Consequently, this criteria promotes solutions where the peak-load units are used only when necessary for ensuring feasibility with respect to the demand constraints (9), and zero values of $Q_j^{\text{peak}}(t)$ otherwise.

The complete continuous-time optimal-control problem with proposed objective function, control variables, constraints and governing dynamic models is given in Appendix A.

Remark 2. *We have imposed the demand satisfaction as hard constraints (9). If upper bounds are imposed on the peak-heating rate (7b), then this formulation may cause feasibility issues. An alternative formulation is to impose these constraints as soft constraints with slack variables penalizing the constraint violation, however, with the associated challenge of designing the penalty function. Similarly, a lower temperature bound T^{min} , imposed as a soft constraint, may be added to (10) for operational resilience, thereby increasing the cluster operator's ability to react upon contingencies in the surplus-heat supply by means of stored heat in the TES unit. A lower temperature-bound may also be necessary to prevent bacteria growth in tank.*

3.2.4. Software Implementation

The system model of the industrial cluster described in the previous section is implemented in the Modelica-based commercial software Dymola (v.2017). To implement the optimal-control problem, we use the Modelica-based open-source platform JModelica.org, version 2.0 [43]. JModelica.org is a versatile platform compliant with Modelica Standard Library, and features interfaces for coupling with many different software packages through Python scripting. JModelica.org incorporates functions for collocation on finite elements for the state and control profiles. To solve the nonlinear programming (NLP), we apply the interior-point NLP solver IPOPT [56] with the MA27 linear solver [57], using the open-source software CasADI [58] for automatic differentiation. For more information, see [59].

The proposed model-based optimization scheme is depicted in Figure 2, showing the connections between the numerical optimization module and the industry cluster and its heat-exchange infrastructure. The control of the pumps, peak-heating units and heat-dumping HEXs is in practice likely to be performed in a receding horizon fashion—see, for instance, [60]. This is illustrated in Figure 2 by the dashed feedback loop. Available measurements from the plants and heat-exchange infrastructure are used to update the current state of the system or initial conditions of the DEAs in problem (A1) as well as the predicted surplus heat and demands. New optimal control-inputs are then computed and applied to the heat-exchange infrastructure. This re-optimization and its frequency, as well as the update of initial conditions and surplus-heat and demand curves, is not further detailed in this paper.

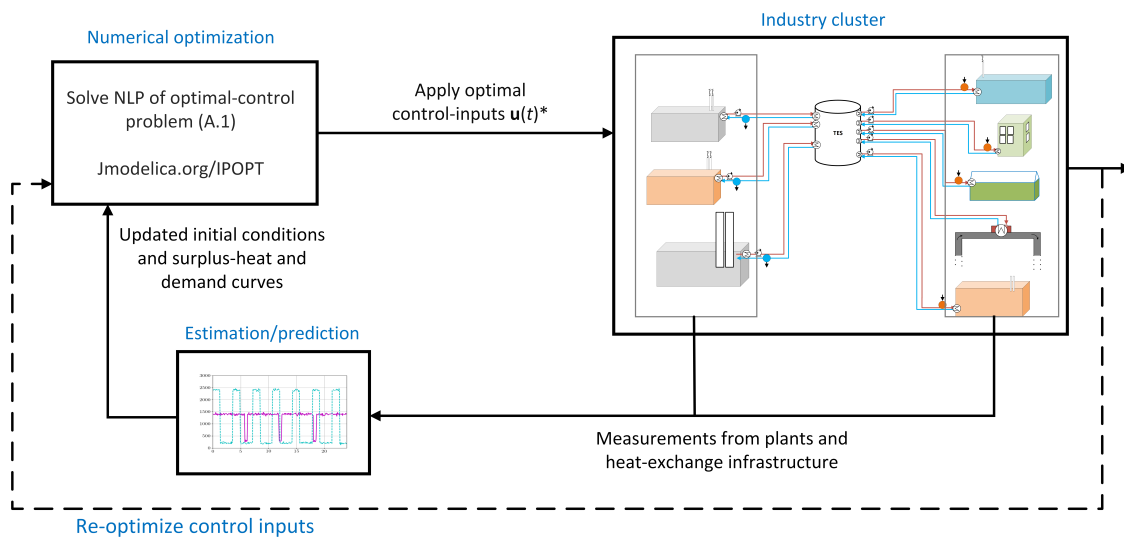


Figure 2. Illustration of the proposed optimal-control scheme.

4. Numerical Case Study

In this section, we demonstrate the proposed modeling and optimization framework on a numerical case study depicted in Figure 3 of an industry cluster with $I = 2$ source plants with surplus heat and $J = 2$ sink plants with heat demands. The surplus heat is assumed to originate from cooling of certain batch processes and be too low-graded for internal use in the plants. Furthermore, the surplus heat from the two plants is assumed to be available as pulses of certain fixed durations as shown in Figure 4. Source plant 1 is assumed to supply a relatively steady heat-flow rate of 1400 kW, while source plant 2 delivers a heat-flow rate of 2400 kW with short durations and high frequency. These characteristics, together with the asynchronous heat demands shown in Figure 5, constitute a challenging heat-exchange control problem.

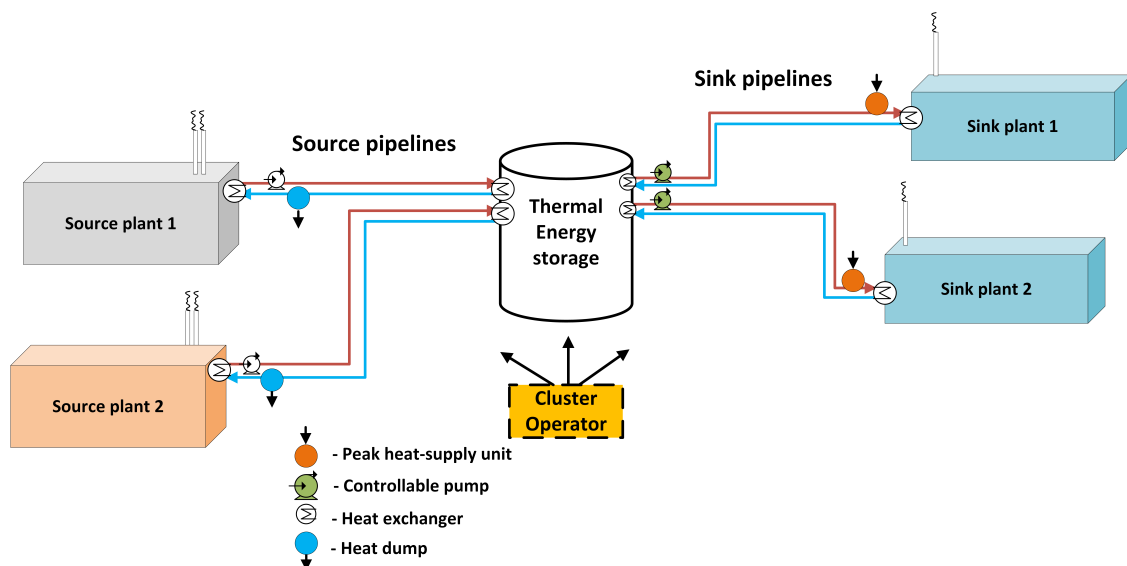


Figure 3. Illustration of industry cluster case study with two source plants with surplus heat and two sink plants with heat demands. The surplus-heat exchange involves intermediate thermal storage controlled by a cluster operator.

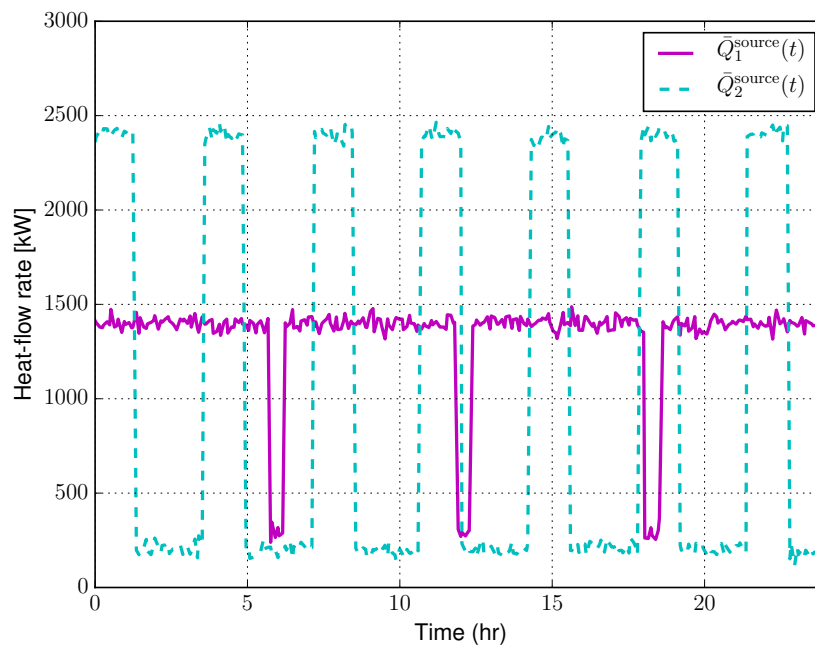


Figure 4. Heat-flow rates from source plants.

For the HEXs between sink pipelines and sink plants, we use $n = 5$ segments and a nominal value of 12 K for LMTD across the HEX, and equally a nominal LMTD of 5 K at the maximum heat-flow rate for the remaining HEXs in the network shown in Figure 3. We set a nominal fluid temperature-glide (trip-return flow) of 12 K through both the source and sink pipelines, from which we together with the maximum demands shown in Figure 5 set the maximum pump flow-rates in (7a) to $\bar{V}_1^{\text{pump}} = 29.9 \times 10^{-3} \text{ m}^3/\text{s}$ and $\bar{V}_2^{\text{pump}} = 41.8 \times 10^{-3} \text{ m}^3/\text{s}$. The maximum return temperature $\bar{T}_i^{\text{source,C}}$ is set to 371 K. Table 3 summarizes values for remaining important parameters used in the case study.

Table 3. Parameter values used in case study.

| Parameter | Value |
|-------------------------------|--|
| t_f | 24 h |
| $\bar{T}_i^{\text{source,C}}$ | 371 K |
| $\bar{T}^{\text{TES,max}}$ | 371 K |
| V^{TES} | 172 m ³ |
| \bar{V}_1^{pump} | $29.9 \times 10^{-3} \text{ m}^3/\text{s}$ |
| \bar{V}_2^{pump} | $41.8 \times 10^{-3} \text{ m}^3/\text{s}$ |
| $(UA)^{\text{loss}}$ | 100 W/K |

Using the TES sizing criteria described in Section 3.1 with a required 1500 kW heat supply for one hour with a maximum 7.5 K temperature drop leads to the volume $V^{\text{TES}} = 172 \text{ m}^3$. We apply a maximum temperature $\bar{T}^{\text{TES,max}} = 371 \text{ K}$, and a nominal temperature $T^{\text{TES,init}} = 362 \text{ K}$. The temperature $\bar{T}_j^{\text{pipe-sink}}$ (boundary condition) at the sink plants is set to 333 K. We assume a 102 m total pipeline length from the source to the sink plants for the supply and return pipelines, respectively, with a pipe diameter of 0.15 m. We set $(UA)^{\text{loss}} = 100 \text{ W/K}$ for the heat loss from the TES unit cf. (3), while we neglect heat losses from the pipelines.

For the optimal-control problem, we set prediction horizon to $t_f = 24 \text{ h}$ and hence assume that surplus-heat streams and the demands vary on a daily basis or shorter period. We set the weights in (12) to $\gamma_1 = 2 \times 10^{-4}$ and $\gamma_2 = 10^{-2}$ upon sufficient scaling of the variables. The allowed deviation δ_j between supplied and demanded heat-flow rate is set to 2.5%. The optimal-control problem (A1) is

infinite dimensional due to the continuous-time system dynamics. To transform the problem into a finite-dimensional NLP problem, we use collocation on finite elements in which the state profiles are approximated by a family of polynomials on finite elements. To this end, we apply three-point Radau collocation in each element, using a total of 100 finite elements. The same discretization approach is applied for the control variables, except for $Q_i^{\text{hd}}(t)$ where we enforce piecewise constant inputs in each element. For details on the discretization scheme, see [61] and [54] (Chapter 10). The resulting NLP has 27,417 variables and 27,422 constraints. Solve times vary between 10 s and 2 min using a standard laptop with Intel Core i7-6600 CPU with 16 GB of RAM.

An important measure for effectiveness of the control scheme's ability to level out offsets in surplus heat and demand is the *total* time-varying surplus and deficit heat in the industry cluster, given as

$$\bar{Q}^{\text{diff}}(t) := \sum_{i \in \mathcal{I}} \bar{Q}_i^{\text{source}}(t) - \sum_{j \in \mathcal{J}} \bar{Q}_j^{\text{demand}}(t), \quad (13a)$$

$$\bar{Q}^{\text{surplus}}(t) := \begin{cases} \bar{Q}^{\text{diff}}(t), & \text{if } \bar{Q}^{\text{diff}}(t) \geq 0, \\ 0, & \text{otherwise,} \end{cases} \quad (13b)$$

$$\bar{Q}^{\text{deficit}}(t) := \begin{cases} |\bar{Q}^{\text{diff}}(t)|, & \text{if } \bar{Q}^{\text{diff}}(t) < 0, \\ 0, & \text{otherwise.} \end{cases} \quad (13c)$$

The total surplus and deficit heat in the four-plant industry cluster, shown in Figure 6, are computed based on the surplus heat shown in Figure 4 and heat demands shown in Figure 5. The time-varying and asynchronous heat supply and demand cause substantial fluctuations in surplus and deficit heat as shown in Figure 6, and hence considerable coordination challenges over the prediction horizon t_i . The total heat demand in the cluster during the 24-h horizon is 56,604 kWh, while available surplus heat is 57,304 kWh. There are five peaks above 2000 kW in deficit heat $\bar{Q}^{\text{deficit}}(t)$, and a total of 15,770 kWh of surplus and 15,070 kWh of deficit heat, respectively. Consequently, the total available surplus heat almost corresponds to the demand, however, with large offsets.

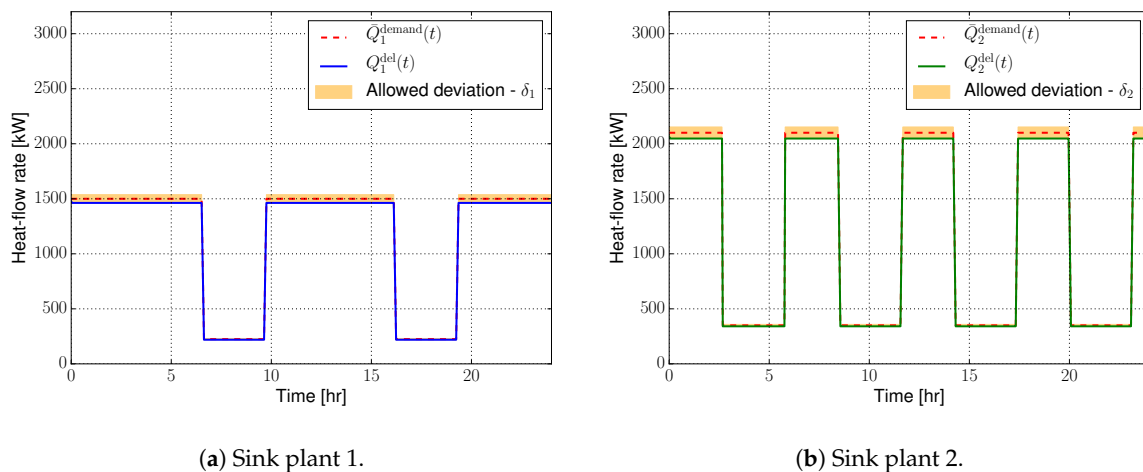


Figure 5. The heat-demands and the actual heat-flow rates into the sink plants for the industry cluster in Figure 3.

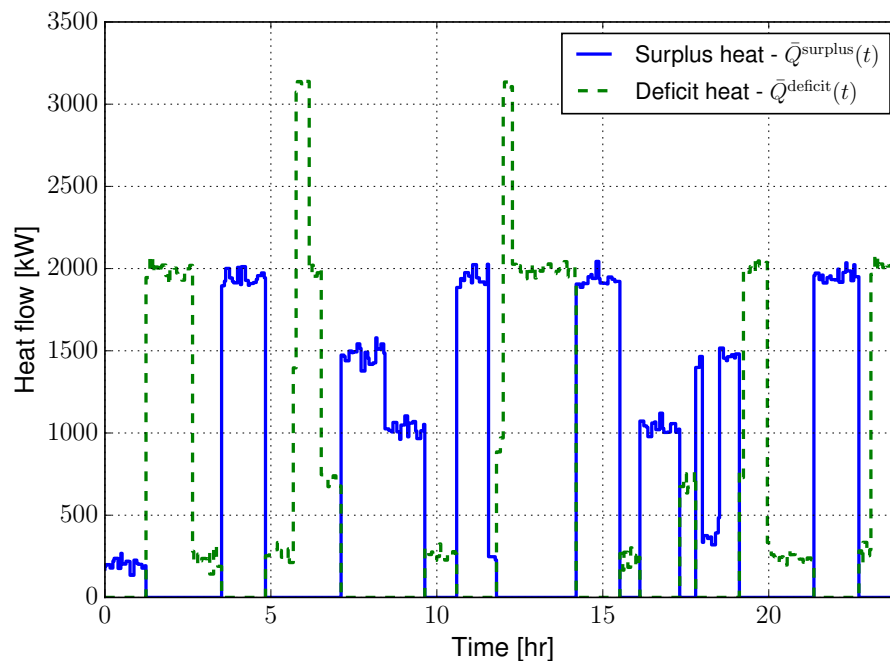


Figure 6. The time-varying total surplus and deficit heat for the industry cluster case study.

4.1. Comparison Case: Surplus-Heat Exchange without TES Unit

To assess the proposed optimal control for the system, we compare the results of the above described case study with a corresponding surplus-heat exchange network shown in Figure 7. The grid is structurally similar to DH networks with single supply and return water pipelines. Each source and sink plant is connected in parallel to the water pipelines, and there is no TES unit. We apply the same optimal-control framework to optimize the surplus-heat exchange of the cluster shown in Figure 7 as described in Section 3.2, that is, with the same set of control variables, objective function and constraints except for the temperature limit on the TES unit. We apply the same modeling scheme for the pipelines and heat exchanger as described in Section 3.1, adapted to the single supply and return pipeline. Note that the pumps connected to each source plant retain fixed flow velocities.

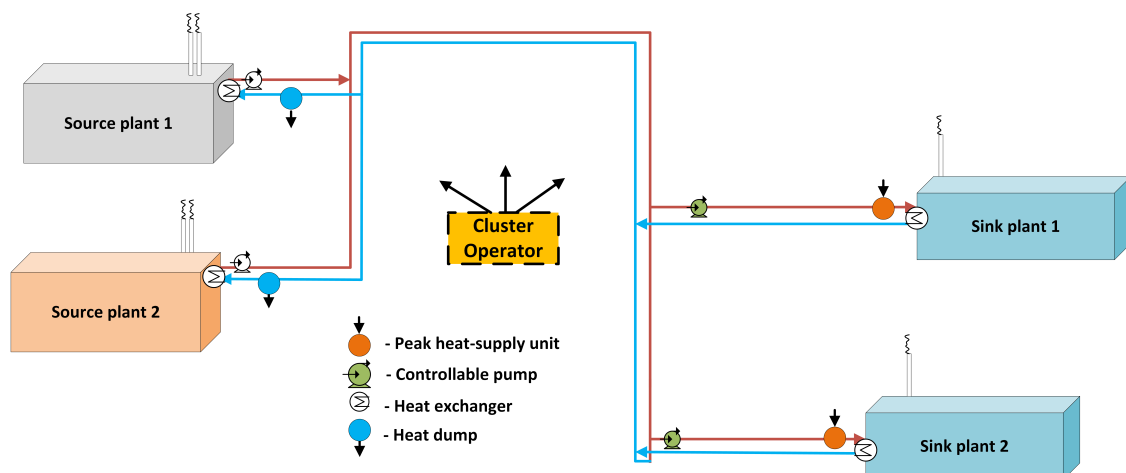


Figure 7. Layout of comparison case consisting of surplus-heat exchange with no thermal storage unit in an industry cluster with two source plants with surplus heat and two sink plants with heat demand.

The main purpose of the comparison is to assess the benefits from combining optimal control *with* thermal energy storage to improve time-varying surplus-heat exchange in industry clusters, as opposed

to optimal control with the thermal storage capacity of the pipelines as the only buffer. Having the same optimal-control problem, we hence use the same total pipeline volume in the networks shown in Figures 3 and 7, respectively. All demands and supplies are identical for the two compared cases.

4.2. Results

Figure 5 displays the time-varying pulse-like heat demands $Q_j^{\text{demand}}(t)$ together with the supplied heat-flow rates for the case with the TES unit shown in Figure 3. A feasible solution is found for the associated NLP of the optimal control problem (A1). This yields heat-flow rates $Q_j^{\text{del}}(t)$, $j = 1, 2$ to the sink plants that are within the allowed deviations δ_j shown by the yellow tubes in Figure 5 as a result of applying the optimal control inputs $\mathbf{u}(t)^*$ to the system. The control inputs are optimal in the sense that the peak-heating supply and the amount of dumped heat is minimized, shown in Figures 8 and 9, respectively, and the pump flow-rates are optimized to utilize the system's available thermal capacities within its given physical and operational constraints (7)–(11). Note that IPOPT is not a global optimization solver. Since the associated NLP from the discretization of optimal control problem (A1) is nonconvex, the obtained solutions are locally but not necessarily globally optimal.

The peak heating necessary to satisfy the sink plants' heat demands in the industry cluster is shown in Figure 8 for the two cases with and without TES. An optimal solution is also found for the NLP of the case without TES, thereby yielding heat-flow rates to the sink plants within the allowed deviations δ_j as shown in Figure 5 for the case with TES unit. Figure 8 displays a substantial difference in the use of peak heating to the meet the plants' demands in the two cases. Out of the five peaks in $\bar{Q}^{\text{deficit}}(t)$ visible in Figure 6, the two peaks in the last part of the horizon are effectively suppressed by optimal utilization of the TES unit. This is achieved by ramping the TES temperature $T^{\text{TES}}(t)$ from around $t = 14.5$ h, cf. Figure 9, after a sustained decrease for about three hours during the long period of deficit heat starting at $t = 11.5$ h. By optimally utilizing the prediction of a peak in deficit heat around $t = 12$ h to ramp up $T^{\text{TES}}(t)$, the operator is able to supply this 3200 kW peak in deficit heat around solely by heat buffered in the TES unit. At this point, $T^{\text{TES}}(t)$ reaches its upper bound (10) as seen in Figure 9. It is the length of this deficit-heat period that causes the maximum peak-heating flow rate of 500 kW around $t = 14$ h. During the 24-h horizon, a total of 895 kWh peak heating is acquired for the case incorporating TES. This constitutes only 5.9% of the total 24 h 15,070 kWh of deficit heat, and means that the operator is able to supply 98.4% of the 57,304 kWh heat demand as surplus heat from the plants in the industry cluster. Observe that the L_1 objective function (12) renders sparse control-input signals $Q_j^{\text{peak}}(t)$, with nonzero peak heating only when necessary to satisfy the demands.

Comparing the case with the industry-cluster structure depicted in Figure 7, i.e., with no TES unit, the sum of peak heating supply essentially follows the pattern of $\bar{Q}^{\text{deficit}}(t)$ in Figure 6. The pipelines are able to buffer only a marginal share of the deficit heat, requiring 13,255 kWh of peak heating which corresponds to 87.9% of the total 15,070 kWh of deficit heat over the 24-h planning horizon. In this case, the operator is only able to supply 76.9% of the 57,304 kWh heat demand as surplus heat from the two source plants. Despite that a large share of the deficit heat must be supplied by peak heating due to lack of a TES unit, the optimal-control scheme is still able to reduce the worst case scenario of 15,070 kWh of daily peak heating with 12.0% or 1815 kWh.

Heat dumping, as displayed in Figure 9 for the case with TES, depends on the storage temperature $T^{\text{TES}}(t)$ and its upper bound (10), as well as the length of periods with surplus heat. As a consequence, the heat dumping is seen to be largest around $t = 12$ h, subsequent to two consecutive periods of surplus heat, during which heat is buffered in the TES unit to minimize the necessary peak heating during the following period of deficit heat. Heat dumping also occurs in relation to the two longer periods of surplus heat seen in Figure 6 around $t = 17$ h and $t = 23$ h. Preventing these periods with heat dumping requires redesigning the TES system, either by changing the volume, temperature level, or pressurization of the tank, or by changing the design of the HEXs between the supply pipelines and the TES. In addition, note that in tuning of the objective function, we have put much lower weight on the heat dumping than the peak heating, assuming access to some cold reservoir. In other cases,

in which cooling is associated with high cost, it may be relevant to penalize heat dumping with a similar magnitude to the penalization of peak heating.

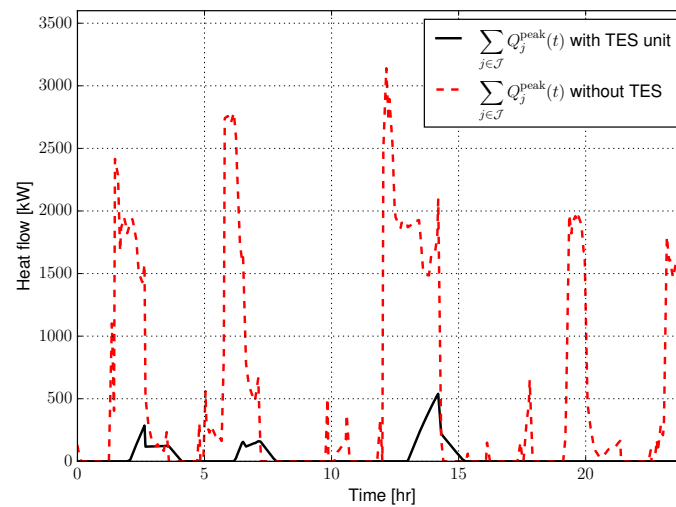


Figure 8. Total peak-heating supply for the case with and without a TES unit.

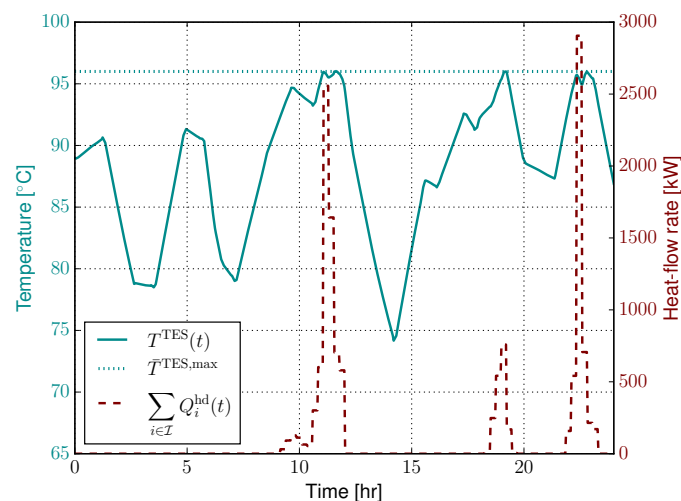


Figure 9. Temperature $T^{\text{TES}}(t)$ in hot water tank (TES unit) and total dumped heat-flow rate $\sum_{i \in \mathcal{I}} Q_i^{\text{hd}}(t)$ for the case in Figure 3 with TES unit.

To assess the impact of size of the hot storage tank constituting the TES unit, we solve the optimal-control problem (A1) for the given time-varying surplus-heat supplies and demands for a set of different storage tank volumes V^{TES} . Figure 10 shows the 24-h total peak heating and total heat dumped, i.e., the integrals of the sums $\sum_{j \in \mathcal{J}} Q_j^{\text{peak}}(t)$ and $\sum_{i \in \mathcal{I}} Q_i^{\text{hd}}(t)$, respectively, and the share of the time $T^{\text{TES}}(t)$ is at its upper bound, as functions of tank volume. The latter metric defines the relative time the TES unit is thermally saturated, in which surplus heat from the two plants cannot be absorbed and must be dumped. The curves for total peak heating and heat dumping both resemble Pareto fronts, where both quantities quickly decay with increasing storage volume. The share of time the storage temperature is saturated is generally low also for small storage volumes, and flattens out around $V^{\text{TES}} = 100 \text{ m}^3$. Above this volume, the TES unit and its HEX design is effective for receiving the two plants' surplus heat for more than 98% of the time. For a given scenario of surplus heat and heat demands, the optimum cost-capacity trade-off of a water-tank TES unit may hence be around the

point at which percentage saturation time flattens out, i.e., a volume somewhat lower than applied in the results shown in Figures 8 and 9. It is important to recall that the design procedure for the TES unit used in the case study does not account for the specific time-variations in surplus and deficit heat. Furthermore, note that the share of time that the TES unit is effective for *delivering* heat to the sink pipelines and plants is not depicted in this figure, but can be extracted from the percentage time peak heating must be supplied as shown in the results in Figure 8.

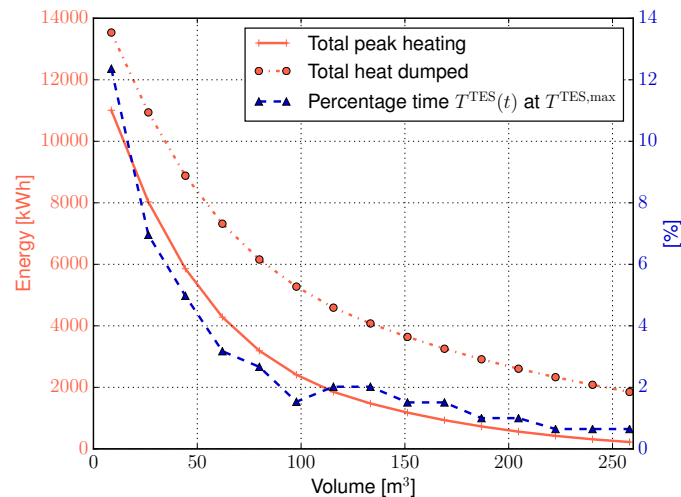


Figure 10. Total peak energy use, total heat dumped (rejected) and total time the storage temperature $T^{\text{TES}}(t)$ is at its upper bound $T^{\text{TES,max}}$ during the 24-h time horizon as a function of TES volume V^{TES} .

5. Conclusions and Future Work

In this paper, we have demonstrated the advantage and importance of optimal control and thermal energy storage to efficiently exploit time-varying surplus heat available in an industry cluster. A case study with two plants with surplus heat available and two plants with a heat demand with and without a TES unit was applied in the study. Our main contribution is the proposed optimal-control scheme, shown through the case study with a TES unit to effectively suppress the use of peak-heating supply through the L_1 penalty formulation, and leverage demand predictions and available thermal storage capacity to mitigate offsets in available surplus heat and demands. Comparison with the case study without a TES unit showed that some but limited amount of the large share of deficit heat resulting from offsets in heat availability and demand could be covered by optimally controlling the pumps and thereby ramp the pipeline temperatures.

Implementation of the proposed scheme would, as briefly outlined in Section 3, typically be through a receding-horizon control policy (MPC). This would introduce feedback and provide a means for accounting for model mismatch and discrepancies in predicted and actual surplus heat and demand. Its use for surplus-heat exchange in industry clusters is, to the best of our knowledge, limited and requires further developing the proposed scheme for improving robustness, numerical efficiency and updating scheme of demand and surplus-heat curves. While these technical as well as other non-technical issues need to be addressed for successful implementation, the proposed scheme addresses important control challenges for heat exchange in industry clusters and thereby provides a direction towards increased inter-plant surplus-heat utilization.

Although we have only considered surplus-heat exchange, the framework may, upon modifications of the governing models and fluid properties, optimize the exchange of other energy flows such as steam and organic rich flue-gases. Furthermore, the optimal control scheme is well suited for incorporating varying peak-heating prices and other means of heat upgrading on the demand side such as heat pumps. The applied fully-mixed hot-water tank should be extended with stratification and possibly hydraulic coupling on the demand side of the tank; this, however, should yield even further

favorable results for the heat-exchange infrastructure with the TES unit. A surplus-heat exchange infrastructure with multiple tanks operating at different temperature levels may also be explored to enable more efficient utilization of different grades of surplus heat. Finally, surplus-heat temperature variations may be accounted for by including the dynamics of the particular cooling processes in the heat source modeling.

Author Contributions: All authors contributed to the model development and analysis of the results. B.R.K. developed and implemented the optimal control problem. B.R.K. wrote the paper, with H.K. and T.A. contributing with reviewing and editing.

Funding: The research leading to this publication has been funded by HighEFF—Centre for an Energy Efficient and Competitive Industry for the Future, an 8-year Research Centre under the FME-scheme (Centre for Environment-friendly Energy Research, 257632/E20). The authors gratefully acknowledge the financial support from the Research Council of Norway and user partners of HighEFF.

Acknowledgments: The authors appreciate valuable inputs from Daniel Rohde, Norwegian University of Science and Technology—NTNU.

Conflicts of Interest: The authors declare no conflict of interest.

Abbreviations and Nomenclature

| | |
|---------------------------|--|
| A | Heat transfer cross area [m ²] |
| amb | Ambient conditions |
| c | Specific heat capacity [kJ/kgK] |
| DAE | Differential algebraic equation |
| DH | District heating |
| del | Delivered |
| HEN | Heat-exchanger network |
| HEX | Heat exchanger |
| hd | Heat dump |
| init | Initial conditions |
| \mathcal{I} | Set of plants with surplus heat |
| \mathcal{J} | Set of plants with heat demand |
| LMTD | Log-mean-temperature-difference |
| loss | Loss to surroundings |
| MPC | Model predictive control |
| NLP | Nonlinear programming |
| n | Number of discrete elements |
| peak | Peak-heating unit |
| pipe-source | heat-transfer pipeline from source plant |
| pipe-sink | heat-transfer pipeline to sink plant |
| Q | Heat-flow rate [kW] |
| \bar{Q}^{source} | Available surplus heat-flow rate from source plant [kW] |
| \bar{Q}^{demand} | Heat demand of sink plant [kW] |
| T | Temperature [K] |
| TES | Thermal energy storage |
| t_f | Prediction horizon of optimal control problem [h] |
| V | Volume [m ³] |
| \dot{V} | Volumetric flow rate [m ³ /s] |
| u | Control input |
| U | Overall heat-transfer coefficient [kW/m ² K] |
| z | Algebraic state of pipeline model |
| δ | Allowed deviation between demanded and supplied heat-flow rate [-] |
| ρ | Density [kg/m ³] |
| γ | Penalty parameter |

Appendix A. Optimal-Control Problem

The complete continuous-time optimal-control problem for the proposed scheme for surplus-heat exchange reads

$$\begin{aligned}
 \min_{\mathbf{u}(t)} \int_{t_0}^{t_f} & \left(\sum_{j \in \mathcal{J}} Q_j^{\text{peak}}(t) + \gamma_1 \sum_{i \in \mathcal{I}} Q_i^{\text{hd}}(t)^2 + \gamma_2 \sum_{j \in \mathcal{J}} v_j^{\text{pump}}(t)^2 \right) dt & (A1) \\
 \text{s.t.} \quad & \left| Q_j^{\text{del}}(t) - \bar{Q}_j^{\text{demand}}(t) \right| \leq \delta_j \bar{Q}_j^{\text{demand}}(t), & j \in \mathcal{J}, \\
 & Q_j^{\text{del}}(t) = Q_j^{\text{TES,out}}(t) - Q_j^{\text{loss}}(t) + Q_j^{\text{peak}}(t), & j \in \mathcal{J}, \\
 & 0 \leq \dot{V}_j^{\text{pump}}(t) \leq \bar{V}_j^{\text{pump}}, & j \in \mathcal{J}, \\
 & Q_j^{\text{peak}}(t) \geq 0, & j \in \mathcal{J}, \\
 & Q_i^{\text{hd}}(t) \leq 0, & i \in \mathcal{I}, \\
 & T^{\text{TES}}(t) \leq \bar{T}^{\text{TES,max}}, \\
 & T_{j,p}^{\text{pipe-source}}(t) \leq \bar{T}_{c,i}^{\text{source}}, & i \in \mathcal{I}, \\
 & \mathbf{F}_i(t, \mathbf{T}_i^{\text{pipe-source}}(t), \mathbf{T}_i^{\text{pipe-source}}(t), \mathbf{z}_i^{\text{pipe-source}}(t), \bar{Q}_i^{\text{source}}(t), Q_i^{\text{TES,in}}(t), Q_i^{\text{loss}}(t), Q_i^{\text{hd}}(t)) = 0, & i \in \mathcal{I}, \\
 & \mathbf{T}_i^{\text{pipe-source}}(0) = \mathbf{T}_i^{\text{pipe-source,init}}, & i \in \mathcal{I}, \\
 & \mathbf{G}_j(t, \mathbf{T}_j^{\text{pipe-sink}}(t), \mathbf{T}_j^{\text{pipe-sink}}(t), \mathbf{z}_j^{\text{pipe-sink}}(t), Q_j^{\text{TES,out}}(t), Q_j^{\text{loss}}(t), \dot{V}_j^{\text{pump}}(t)) = 0, & j \in \mathcal{J}, \\
 & \mathbf{T}_j^{\text{pipe-sink}}(0) = \mathbf{T}_j^{\text{pipe-sink,init}}, & j \in \mathcal{J}, \\
 & \rho c^{\text{w}} V^{\text{TES}} \dot{T}^{\text{TES}}(t) = \sum_{i \in \mathcal{I}} Q_i^{\text{TES,in}}(t) - \sum_{j \in \mathcal{J}} Q_j^{\text{TES,out}}(t) - Q^{\text{TES,loss}}(t), \\
 & T^{\text{TES}}(0) = T^{\text{TES,init}}.
 \end{aligned}$$

The vector of control variables $\mathbf{u}(t)$ is defined in Equation (6).

References

1. Figueres, C.; Schellnhuber, H.J.; Whiteman, G.; Rockström, J.; Hobley, A.; Rahmstorf, S. Three years to safeguard our climate. *Nature* **2017**, *546*, 593–595. [CrossRef]
2. SPIRE. SPIRE Roadmap. *Sustainable Process Industry through Resource and Energy Efficiency*; Technical Report; SPIRE: Brussels, Belgium, 2013.
3. Huang, F.; Zheng, J.; Baleynaud, J.M.; Lu, J. Heat recovery potentials and technologies in industrial zones. *J. Energy Inst.* **2017**, *90*, 951–961. [CrossRef]
4. Chertow, M.R. “Uncovering” Industrial Symbiosis. *J. Ind. Ecol.* **2007**, *11*, 11–30. [CrossRef]
5. Klemeš, J.J.; Kravanja, Z. Forty years of Heat Integration: Pinch analysis (PA) and Mathematical Programming (MP). *Curr. Opin. Chem. Eng.* **2013**, *2*, 461–474. [CrossRef]
6. Yee, T.F.; Grossmann, I.E. Simultaneous optimization models for heat integration II: Heat exchanger network synthesis. *Comput. Chem. Eng.* **1990**, *14*, 1165–1184. [CrossRef]
7. Boix, M.; Montastruc, L.; Azzaro-Pantel, C.; Domenech, S. Optimization methods applied to the design of eco-industrial parks: A literature review. *J. Clean. Prod.* **2015**, *87*, 303–317. [CrossRef]
8. Dal Magro, F.; Meneghetti, A.; Nardin, G.; Savino, S. Enhancing energy recovery in the steel industry: Matching continuous charge with off-gas variability smoothing. *Energy Convers. Manag.* **2015**, *104*, 78–89. [CrossRef]
9. Hiete, M.; Ludwig, J.; Schultmann, F. Intercompany Energy Integration: Adaptation of Thermal Pinch Analysis and Allocation of Savings. *J. Ind. Ecol.* **2012**, *16*, 689–698. [CrossRef]
10. Jiménez-Arreola, M.; Pili, R.; Dal, F.; Wieland, C.; Rajoo, S.; Romagnoli, A. Thermal power fluctuations in waste heat to power systems: An overview on the challenges and current solutions. *Appl. Therm. Eng.* **2018**, *134*, 576–584. [CrossRef]

11. Aguilera, N.; Marchetti, J.L. Optimizing and controlling the operation of heat-exchanger networks. *AIChE J.* **1998**, *44*, 1090–1104. [[CrossRef](#)]
12. González, A.H.; Odloak, D.; Marchetti, J.L. Predictive control applied to heat-exchanger networks. *Chem. Eng. Process. Process Intensif.* **2006**, *45*, 661–671. [[CrossRef](#)]
13. Bakošová, M.; Oravec, J. Robust model predictive control for heat exchanger network. *Appl. Therm. Eng.* **2014**, *73*, 924–930. [[CrossRef](#)]
14. Oravec, J.; Bakošová, M.; Trafczynski, M.; Vasičkaninová, A.; Mészáros, A.; Markowski, M. Robust model predictive control and PID control of shell-and-tube heat exchangers. *Energy* **2018**, *159*, 1–10. [[CrossRef](#)]
15. Vasičkaninová, A.; Bakošová, M. Control of a heat exchanger using neural network predictive controller combined with auxiliary fuzzy controller. *Appl. Therm. Eng.* **2015**, *89*, 1046–1053. [[CrossRef](#)]
16. Sun, K.; Tseng, C.T.; Wong, D.S.H.; Shieh, S.S.; Jang, S.S.; Kang, J.L.; Hsieh, W.D. Model predictive control for improving waste heat recovery in coke dry quenching processes. *Energy* **2015**, *80*, 275–283. [[CrossRef](#)]
17. Wang, X.; Palazoglu, A.; El-farra, N.H. Proactive optimization and control of heat-exchanger super networks. *IFAC-PapersOnLine* **2015**, *48*, 593–598. [[CrossRef](#)]
18. Glemmestad, B.; Skogestad, S.; Gundersen, T. Optimal operation of heat exchanger networks. *Comput. Chem. Eng.* **1999**, *23*, 509–522. [[CrossRef](#)]
19. Jäschke, J.; Skogestad, S. Optimal operation of heat exchanger networks with stream split: Only temperature measurements are required. *Comput. Chem. Eng.* **2014**, *70*, 35–49. [[CrossRef](#)]
20. Scholten, T.; De Persis, C.; Tesi, P. Modeling and Control of Heat Networks with Storage: The Single-Producer Multiple-Consumer Case. *IEEE Trans. Control Syst. Technol.* **2017**, *25*, 414–428. [[CrossRef](#)]
21. Sun, L.; Zha, X.; Luo, X. Coordination between bypass control and economic optimization for heat exchanger network. *Energy* **2018**, *160*, 318–329. [[CrossRef](#)]
22. Jin, Y.; Gao, N.; Zhu, T. Controlled variable analysis of counter flow heat exchangers based on thermodynamic derivation. *Appl. Therm. Eng.* **2018**, *129*, 684–692. [[CrossRef](#)]
23. Bonilla, J.; Roca, L. Model validation and control strategy of a heat recovery system integrated in a renewable hybrid power plant demonstrator. *Sol. Energy* **2018**, *176*, 698–708. [[CrossRef](#)]
24. Schumm, G.; Philipp, M.; Schlosser, F.; Hesselbach, J.; Walmsley, T.G.; Atkins, M.J. Hybrid heating system for increased energy efficiency and flexible control of low temperature heat. *Energy Effic.* **2018**, *11*, 1117–1133. [[CrossRef](#)]
25. Walmsley, T.G.; Walmsley, M.R.W.; Atkins, M.J.; Neale, J.R. Integration of industrial solar and gaseous waste heat into heat recovery loops using constant and variable temperature storage. *Energy* **2014**, *75*, 53–67. [[CrossRef](#)]
26. Chen, Q.; Zhang, M.Q.; Dong, E.F.; Wang, Y.F.; Sui, Y.Q. Reliable simultaneous operation strategy in heat exchanger networks under variable heat loads. *Appl. Therm. Eng.* **2019**, *149*, 1125–1133. [[CrossRef](#)]
27. Sunil, P.U.; Barve, J.; Nataraj, P.S.V. A robust heat recovery steam generator drum level control for wide range operation flexibility considering renewable energy integration. *Energy* **2018**, *163*, 873–893. [[CrossRef](#)]
28. Atkins, M.J.; Walmsley, M.R.W.; Neale, J.R. Process integration between individual plants at a large dairy factory by the application of heat recovery loops and transient stream analysis. *J. Clean. Prod.* **2012**, *34*, 21–28. [[CrossRef](#)]
29. Wang, Y.; You, S.; Zheng, W.; Zhang, H.; Zheng, X.; Miao, Q. State space model and robust control of plate heat exchanger for dynamic performance improvement. *Appl. Therm. Eng.* **2018**, *128*, 1588–1604. [[CrossRef](#)]
30. Whalley, R.; Ebrahimi, K.M. Heat exchanger dynamic analysis. *Appl. Math. Model.* **2018**, *62*, 38–50. [[CrossRef](#)]
31. Chang, H.H.; Chang, C.T.; Li, B.H. Game-theory based optimization strategies for stepwise development of indirect interplant heat integration plans. *Energy* **2018**, *148*, 90–111. [[CrossRef](#)]
32. Gu, S.; Liu, L.; Zhang, L.; Bai, Y.; Wang, S.; Du, J. Heat exchanger network synthesis integrated with flexibility and controllability. *Chin. J. Chem. Eng.* **2018**, in press. [[CrossRef](#)]
33. Čuček, L.; Boldyryev, S.; Klemeš, J.J.; Kravanja, Z.; Krajačić, G.; Varbanov, P.S.; Duić, N. Approaches for retrofitting heat exchanger networks within processes and Total Sites. *J. Clean. Prod.* **2019**, *211*, 884–894. [[CrossRef](#)]

34. Schlosser, F.; Peesel, R.H.; Meschede, H.; Philipp, M.; Walmsley, T.G.; Walmsley, M.R.W.; Atkins, M.J. Design of Robust Total Site Heat Recovery Loops via Monte Carlo Simulation. *Energies* **2019**, *12*, 930. [[CrossRef](#)]
35. Zhang, C.; Zhou, L.; Chhabra, P.; Garud, S.S.; Aditya, K.; Romagnoli, A.; Comodi, G.; Dal Magro, F.; Meneghetti, A.; Kraft, M. A novel methodology for the design of waste heat recovery network in eco-industrial park using techno-economic analysis and multi-objective optimization. *Appl. Energy* **2016**, *184*, 88–102. [[CrossRef](#)]
36. Hassiba, R.J.; Al-Mohannadi, D.M.; Linke, P. Carbon dioxide and heat integration of industrial parks. *J. Clean. Prod.* **2017**, *155*, 47–56. [[CrossRef](#)]
37. Roberts, B.H. The application of industrial ecology principles and planning guidelines for the development of eco-industrial parks: An Australian case study. *J. Clean. Prod.* **2004**, *12*, 997–1010. [[CrossRef](#)]
38. Eynard, J.; Grieu, S.; Polit, M. Predictive control and thermal energy storage for optimizing a multi-energy district boiler. *J. Process Control* **2012**, *22*, 1246–1255. [[CrossRef](#)]
39. Fritszon, P.; Bunuş, P. Modelica—A General Object-Oriented Language for Continuous and Discrete-Event System Modeling and Simulation. In Proceedings of the 35th Annual Simulation Symposium, San Diego, CA, USA, 14–18 April 2002.
40. Schweiger, G.; Larsson, P.O.; Magnusson, F.; Lauenburg, P.; Velut, S. District heating and cooling systems—Framework for Modelica-based simulation and dynamic optimization. *Energy* **2017**, *137*, 566–578. [[CrossRef](#)]
41. Kauko, H.; Kvalsvik, K.H.; Rohde, D.; Nord, N.; Utne, Å. Dynamic modeling of local district heating grids with prosumers: A case study for Norway. *Energy* **2018**, *151*, 261–271. [[CrossRef](#)]
42. Rohde, D.; Andresen, T.; Nord, N. Analysis of an integrated heating and cooling system for a building complex with focus on long-term thermal storage. *Appl. Therm. Eng.* **2018**, *145*, 791–803. [[CrossRef](#)]
43. Åkesson, J.; Årzén, K.E.; Gäfvert, M.; Bergdahl, T.; Tummescheit, H. Modeling and optimization with Optimica and JModelica.org—Languages and tools for solving large-scale dynamic optimization problems. *Comput. Chem. Eng.* **2010**, *34*, 1737–1749. [[CrossRef](#)]
44. Soons, F.; Torrens, J.I.; Hensen, J.; Schrevel, R.D. A Modelica based computational model for evaluating a renewable district heating system. In Proceedings of the 9th International Conference on System Simulation in Buildings, Liege, Belgium, 10–12 December 2014.
45. Strikwerda, J. *Finite Difference Schemes and Partial Differential Equations*, 2nd ed.; SIAM: Philadelphia, PA, USA, 2004.
46. International Energy Agency. *Energy Storage Technology Roadmap: Technology Annex*; Technical Report; International Energy Agency (IEA): Paris, France, 2014.
47. Caldwell, J.S.; Bahnfleth, W.P. Identification of mixing effects in stratified chilled-water storage tanks by analysis of time series temperature data. *ASHRAE Trans.* **1998**, *104*, 366–376.
48. Han, Y.M.; Wang, R.Z.; Dai, Y.J. Thermal stratification within the water tank. *Renew. Sustain. Energy Rev.* **2009**, *13*, 1014–1026. [[CrossRef](#)]
49. Miró, L.; Gasia, J.; Cabeza, L.F. Thermal energy storage (TES) for industrial waste heat (IWH) recovery: A review. *Appl. Energy* **2016**, *179*, 284–301. [[CrossRef](#)]
50. Incropera, F.P.; Dewitt, D.P.; Bergman, T.L.; Lavine, A.S. *Principles of Heat and Mass Transfer*; Wiley: New York, NY, USA, 2013.
51. Wang, H.; Lahdelma, R.; Wang, X.; Jiao, W.; Zhu, C. Analysis of the location for peak heating in CHP based combined district heating systems. *Appl. Therm. Eng.* **2015**, *87*, 402–411. [[CrossRef](#)]
52. Timmerman, J.; Hennen, M.; Bardow, A.; Lodewijks, P.; Vandeveld, L.; Eetvelde, G.V. Towards low carbon business park energy systems: A holistic techno-economic optimisation model. *Energy* **2017**, *125*, 747–770. [[CrossRef](#)]
53. Jose, P. Stochastic Unit Commitment and Self-scheduling: A Review Considering CO₂ Emission Modeling. In *Handbook of CO₂ in Power Systems Energy Systems*; Zheng, Q.P., Rebennack, S., Pardalos, P.M., Pereira, M.V.F., Iliadis, N.A., Eds.; Energy Systems; Springer: Berlin/Heidelberg, Germany, 2012; pp. 311–326.
54. Biegler, L.T. *Nonlinear Programming: Concepts, Algorithms, and Applications to Chemical Processes*; SIAM: Philadelphia, PA, USA, 2010.

55. Candes, E.J.; Wakin, M.B.; Boyd, S.P. Enhancing sparsity by reweighted L_1 minimization. *J. Fourier Anal. Appl.* **2008**, *14*, 877–905. [[CrossRef](#)]
56. Wächter, A.; Biegler, L.T. On the implementation of an interior-point filter line-search algorithm for large-scale nonlinear programming. *Math. Program.* **2005**, *106*, 25–57. [[CrossRef](#)]
57. HSL. A Collection of Fortran Codes for Large Scale Scientific Computation. 2018. Available online: <http://www.hsl.rl.ac.uk/> (accessed on 15 May 2017).
58. Andersson, J.; Åkesson, J.; Diehl, M. CasADi: A Symbolic Package for Automatic Differentiation and Optimal Control. In *Recent Advances in Algorithmic Differentiation*; Forth, S., Hovland, P., Phipps, E., Utke, J., Walther, A., Eds.; Springer: Berlin/Heidelberg, Germany, 2012; pp. 297–307. [[CrossRef](#)]
59. Magnusson, F.; Åkesson, J. Dynamic Optimization in JModelica.org. *Processes* **2015**, *3*, 471–496. [[CrossRef](#)]
60. Rawlings, J.; Mayne, D. *Model Predictive Control: Theory and Design*; Nob Hill Publishing: Madison, WI, USA, 2009.
61. Magnusson, F.; Åkesson, J. Collocation methods for optimization in a Modelica environment. In Proceedings of the 9th International Modelica Conference, Munich, Germany, 3–5 September 2012; pp. 649–658.



© 2019 by the authors. Licensee MDPI, Basel, Switzerland. This article is an open access article distributed under the terms and conditions of the Creative Commons Attribution (CC BY) license (<http://creativecommons.org/licenses/by/4.0/>).